Bits, Channels, Frequencies and Unlimited Sensing: Pushing the Limits of Sub-Nyquist Prony

Václav Pavlíček, Ruiming Guo and Ayush Bhandari
Dept. of Electrical and Electronic Engg., Imperial College London, SW7 2AZ, UK.
vaclav.pavlicek20,ruiming.guo,a.bhandari {@imperial.ac.uk}

***Abstract*—Parametric sampling of complex exponentials is a problem widely studied in harmonic analysis and it has wide applications in radar, communications, near-far and other fields. One of the approaches to estimating complex exponentials is Prony's method which allows estimation of K exponentials from $2K$ samples. In practice during digital acquisition using Shannon's framework, the amplitude is bounded by the dynamic range of the ADC. This is overcome by the Unlimited Sensing Framework. In this paper, we propose an approach that mimics Prony's method and can estimate the parameters of complex exponentials without any sampling rate requirements from $6K$ samples. This strategy uses multi-channel USF architecture that can implement either real-valued or complex-valued thresholds based on Gaussian integers. Lastly, we present the effect of quantization noise on the performance of both estimation strategies, and calculate the Effective Number of Bits and show that four quantization bits are sufficient for sub-Nyquist frequency estimation.**

***Index Terms*—USF, Sub-Nyquist Spectral Estimation, Quantization**

I. Introduction

Frequency or spectral estimation plays a key role in signal processing [1], [2], finding applications in radar systems, digital communications, time-of-flight imaging, and the near-far problem. Its origins can be traced back to the 18th century with Prony's method, which facilitates the estimation of K frequencies from $2K$ samples, given a sufficiently small sampling step. However, Analog-to-Digital Converters (ADCs) adhering to the Shannon-Nyquist Framework set limits on the sampling rate. These limits pose challenges in higher frequency bands, necessitating the adoption of sub-Nyquist frequency estimation. These methods can be broadly classified into two groups: (i) stochastic methods, which use coprime samplers and statistical recovery techniques [3], [4]; and (ii) deterministic methods, based on the Chinese Remainder Theorem (CRT) and Robust CRT (RCRT) [5]. These techniques share a foundational reliance on model assumptions and the principle of pointwise sampling as prescribed by the Shannon-Nyquist framework. However, in practice, ADCs are limited by constraints such as limited dynamic range (DR) and digital resolution (DRes)—stemming from a fixed bit budget and quantization—pose significant challenges, resulting in permanent loss of information.

The work of the authors is supported by the UK Research and Innovation council's FLF Program "Sensing Beyond Barriers via Non-Linearities" (MRC Fellowship award no. MR/Y003926/1). Further details on Unlimited Sensing and upcoming materials on *reproducible research* are available via `https://bit.ly/USF-Link`.

To overcome these fundamental limitations in DR and DRes, the Unlimited Sensing Framework (USF) has been recently introduced [6] as an alternative method. The USF adopts a radically different approach to sampling theory, basing itself on a synergistic co-design of hardware and software. By integrating modulo folding into the analog hardware, it avoids clipping and saturation, thus achieving a higher digital resolution within a specified bit budget. Subsequently, specialized recovery algorithms are developed to effectively invert the folded samples, enabling High Dynamic Range (HDR) signal reconstruction.

Given the recency of the USF, much of the research in sampling theory has centered on bandlimited signal classes [7]–[10]. While prior works have explored time domain and frequency domain sparse signals [11]–[14], their scope has been confined mainly to single-channel architectures. This approach necessitates oversampling for inversion of modulo folding, which contradicts the sub-Nyquist ethos of spectral estimation problem.

Multi-channel USF (MC-USF) [15]–[18] utilizing irrational ratio of modulo thresholds for CRT-based recovery have recently emerged, particularly for bandlimited signals [15], [16]. However, these works do not extend to sub-Nyquist frequency estimation. Our research builds upon ongoing efforts [19] to formulate a deterministic strategy for sub-Nyquist frequency estimation within the USF architecture, also using irrational threshold ratios. While the work in [19] incorporates hardware validation, it does not address the analysis of quantization noise.

Contributions. The current paper makes the following contributions: (C_1) A new MC-USF acquisition architecture that allows for sub-Nyquist frequency estimation is presented, (C_2) A new recovery algorithm for sub-Nyquist frequency estimation is proposed, and (C_3) Analysis of the effect of the quantization noise on the robustness of the recovery algorithm is considered.

Notation. The set of integer, real, and complex-valued numbers are denoted by $\mathbb{Z}, \mathbb{R}$, and $\mathbb{C}$, respectively. The set of N integers is given by $\mathbb{I}_N = \{0, \cdots, N-1\}, N \in \mathbb{Z}^+$. The conjugate of $z \in \mathbb{C}$ is denoted by z^*. Continuous function and its discrete counterpart are written as $g(t), t \in \mathbb{R}$ and $g[n], n \in \mathbb{Z}$, respectively. $\Re(z)$ denotes the real part of a complex number and $\Im(z)$ stands for the imaginary part. The greatest common divisor of $p, q \in \mathbb{Z}$ is denoted as $\mathtt{GCD}(p,q)$ and the least common multiple is denoted as $\mathtt{LCM}(p,q)$. Gaussian integer ($\mathtt{GI}$) is defined as $\tau(p,q) = p + \jmath q, p, q \in \mathbb{Z}$. The max-norm of a function is defined as, $\|g\|_\infty = \inf\{c_0 \geqslant 0 : |g(t)| \leqslant c_0\}$; for sequences, we use, $\|g\|_\infty = \max_n |g[n]|$. The zero-centred

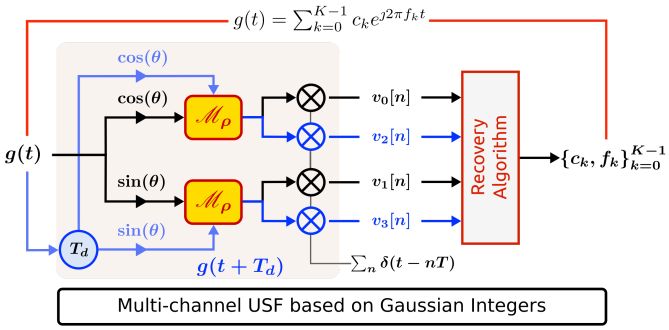

Fig. 1. USF acquisition architecture with Gaussian integer thresholds that allows sub-Nyquist frequency estimation.

modulo operator is defined as

$$\mathscr{M}_\lambda : g \mapsto 2\lambda \left(\left[\!\left[\frac{g}{2\lambda} + \frac{(1+\jmath)}{2} \right]\!\right] - \frac{(1+\jmath)}{2} \right), \ \lambda \in \mathbb{C} \quad (1)$$

where $[\![g]\!] \stackrel{\text{def}}{=} g - (\lfloor \Re(g) \rfloor + \jmath \lfloor \Im(g) \rfloor)$ and $\lfloor \cdot \rfloor$ denotes the floor operation. The quantization operator is defined as $\mathscr{Q}(g) = \lfloor g + \frac{1}{2} \rfloor, g \in \mathbb{R}$. The mean-square error (MSE) between $\mathbf{x}, \mathbf{y} \in \mathbb{R}^N$ is denoted as $\mathcal{E}_2(\mathbf{x}, \mathbf{y}) \stackrel{\text{def}}{=} \frac{1}{N} \sum_{n=0}^{N-1} |x[n] - y[n]|^2$.

II. Sub-Nyquist USF Spectral Estimation

In order to invoke the true flavour of sub-Nyquist USF, we propose a novel sampling architecture utilizing Gaussian-integers that results in an *exact* spectral estimation from as few as $6K$ folded samples. Before we state the sampling theorem, we first present the problem formulation and notations needed.

Problem Formulation. Let the input signal $g(t)$ be a finite sum of K complex exponentials,

$$g(t) = \sum\nolimits_{k=0}^{K-1} c_k e^{\jmath \omega_k t}, \ \omega_k = 2\pi f_k, \quad (2)$$

where c_k, ω_k are the unknown amplitude and frequency of interest, respectively. We assume a real-valued input $g(t)$ that matches the practical scenarios. The proposed MC-USF architecture is concretely depicted in Fig. 1.

Let $\lambda = \epsilon \tau(p, q) = 2\rho e^{-\jmath \theta}$ be a scaled GI, where $\epsilon \in \mathbb{R}^+$. The key feature of this sampling paradigm is that, 1) quadrature sampling is utilized to implement the complex-valued modulo operation, and 2) the continuous-time signal is first folded via non-linear modulo operation, and then sampled in a pointwise fashion, resulting in a low-dynamic-range (LDR) folded measurements which can be characterized as

$$\begin{bmatrix} v_0[n] & v_1[n] \\ v_2[n] & v_3[n] \end{bmatrix} = \mathscr{M}_\rho \left(\begin{bmatrix} g[n] \\ g_{T_d}[n] \end{bmatrix} \begin{bmatrix} \cos\theta & \sin\theta \end{bmatrix} \right) \quad (3)$$

where $g[n] = g(nT)$, $g_{T_d}[n] = g(nT + T_d)$ and T_d is the time delay, $T = 1/f_s$ is the sampling step and $f_s \ll f_{\max}, f_{\max} = \|f_k\|_\infty$. That said, the measurements $\{v_l[n]\}_{n \in \mathbb{I}_{N_l}}^{l \in \mathbb{I}_4}$ are folded in both amplitude and frequency domain. Given the multi-channel measurements $\{v_l[n]\}_{n \in \mathbb{I}_{N_l}}^{l \in \mathbb{I}_4}$, our goal is to design a theoretically guaranteed recovery approach that retrieves the signal parameters $\{c_k, f_k\}_{k \in \mathbb{I}_K}$.

CRT-based Sub-Nyquist USF Spectral Estimation. The concurrent modulo non-linearity cannot be inverted via techniques inherently designed for single-channel modulo samples, such as non-linear filtering of amplitudes [6] or by Fourier-domain separation proposed in [7], since each channel measurement is undersampled. Nonetheless, common to the idea in [17], [19], the channel redundancy across $\{v_l[n]\}_{n \in \mathbb{I}_{N_l}}^{l \in \mathbb{I}_4}$ allows for amplitude unfolding via CRT under appropriate choice on λ.

The key insight being that $\{v_0[n]\}_{n \in \mathbb{I}_{N_0}}$ and $\{v_1[n]\}_{n \in \mathbb{I}_{N_1}}$ ($\{v_2[n]\}_{n \in \mathbb{I}_{N_2}}$ and $\{v_3[n]\}_{n \in \mathbb{I}_{N_3}}$) share the same input signal $g(t)$ ($g(t + T_d)$) that is quadrature sampled (see (3)), its combination results in the system of congruence equations, *i.e.*,

$$\begin{cases} g[n] = \epsilon (\theta_0[n] + \jmath \theta_1[n]) (p + \jmath q) + r_0[n] \\ g[n] = \epsilon (\phi_0[n] + \jmath \phi_1[n]) (p - \jmath q) + r_1[n] \end{cases}, \quad (4)$$

where $\{\theta_l[n], \phi_l[n]\} \in \mathbb{Z}^2, n \in \mathbb{I}_{N_l}, l \in \mathbb{I}_2$, and $r_0[n] = r_1^*[n] = (v_0[n] + \jmath v_1[n]) e^{-\jmath \theta}$. Notice that, $\mathrm{GCD}(p, q) = 1$. Hence, $\{v_0[n]\}_{n \in \mathbb{I}_{N_0}}$ and $\{v_1[n]\}_{n \in \mathbb{I}_{N_1}}$ provide for $\{g[n]\}_{n \in \mathbb{I}_N}$ due to the GI structure, *viz.* $\lambda = \epsilon(p + \jmath q)$. This allows for amplitude unfolding that is independent of any sampling rate requirement, provided that $\|g(t)\|_\infty < \epsilon \frac{p^2 + q^2}{2}$.

Our main result is summarized as follows.

Theorem 1. *Let $g(t) = \sum_{k=0}^{K-1} c_k e^{\jmath \omega_k t}$. Given multi-channel modulo samples $\{v_l[n]\}_{n \in \mathbb{I}_{N_l}}^{l \in \mathbb{I}_4}$ defined in* (3)*. Then, $g(t)$ can be exactly recovered with $N_l \geqslant \left(2 - \lfloor \frac{l}{2} \rfloor\right) K, l \in \mathbb{I}_4$ samples if $\mathrm{GCD}(p, q) = 1$, $T_d \leqslant \frac{\pi}{\max_k |\omega_k|}$ and $\|g(t)\|_\infty < \epsilon \frac{p^2 + q^2}{2}$.*

Proof. Our proof is constructive and decouples the concurrent inversions of amplitude and frequency folding.

Amplitude Unfolding. We first unfold the amplitude utilizing the CRT [20]. From (3) and sampling architecture, we can write down the following linear congruence equations as,

$$\epsilon \begin{bmatrix} p & -q & 0 & 0 \\ q & p & 0 & 0 \\ 0 & 0 & p & q \\ 0 & 0 & -q & p \end{bmatrix} \begin{bmatrix} \theta_0 \\ \theta_1 \\ \phi_0 \\ \phi_1 \end{bmatrix} + \begin{bmatrix} \Re(r_0[n]) \\ \Im(r_0[n]) \\ \Re(r_1[n]) \\ \Im(r_1[n]) \end{bmatrix} = \begin{bmatrix} \Re(g[n]) \\ \Im(g[n]) \\ \Re[g[n]] \\ \Im(g[n]) \end{bmatrix}. \quad (5)$$

Given the integer constraints on $\{\theta_l[n], \phi_l[n]\} \in \mathbb{Z}^2, n \in \mathbb{I}_{N_l}$ and $\|g(t)\|_\infty < \epsilon(p^2 + q^2)/2$, then $\{\theta_l[n], \phi_l[n]\}, n \in \mathbb{I}_{N_l}$ can be uniquely determined using exhaustive search.

Frequency Unfolding. Let $\nu_k = \mathscr{M}_{f_s/2}(f_k)$ be the aliased frequency of f_k. Then, the samples can be written as,

$$\begin{cases} g[n] = \sum_{k=0}^{K-1} c_k e^{\jmath 2\pi \frac{\nu_k}{f_s} n} \\ g_{T_d}[n] = \sum_{k=0}^{K-1} c_k e^{\jmath 2\pi f_k T_d} e^{\jmath 2\pi \frac{\nu_k}{f_s} n} \end{cases}. \quad (6)$$

The common frequency components of $g[n]$ and $g_{T_d}[n]$ can be estimated using Prony's method as follows. Let $h[n]$ be a filter with z-transform $h(z) = \sum_{n=0}^{K} h[n] z^{-n} = \prod_{k=0}^{K-1} (1 - u_k z^{-1})$ denote the z-transform where its roots are $u_k = e^{\jmath 2\pi \nu_k / f_s}$. The filter $h[n]$ annihilates $g[n]$ such that $(g * h)[n] = \sum_{k=0}^{K-1} c_k u_k^n \sum_{m=0}^{K} h[m] u_k^{-m} = 0, K \leqslant n \leqslant N - 1$. This can be algebraically rewritten in the matrix form as $\mathbf{T}(g)\mathbf{h} = \mathbf{0}$, where $\mathbf{T}(g)$ is a $(N - K) \times (K + 1)$ Toeplitz matrix constructed by $\{g[n]\}_{n \in \mathbb{I}_N}$. To solve these linear equations, there should be at least as many equations as unknowns, *i.e.*, $N \geqslant 2K$. This leads to the condition, $N_0, N_1 \geqslant 2K$. Amplitudes c_k can be found using the least squares (LS) method. Anti-aliased frequencies f_k can be estimated from the phase term $e^{\jmath 2\pi f_k T_d}$ by utilizing LS method from (6), resulting in $N_2, N_3 \geqslant K$ since $\{\nu_k\}_{k\in\mathbb{I}_K}$ is common to all channels. This completes the proof of the theorem. $\square$

Compared to [15], [19], we have the following results:

Remark 1. *The design of multi-channel sampling architecture allows for a reduction of the number of ADCs by half compared to [15] for real-valued input.*

Remark 2. *In contrast to [19], the architecture proposed in Fig. 1 operates directly in the sample domain, and therefore 1) it can estimate DC value, and 2) and requires only $6K$ samples in total smaller than $6K + 4$ samples in [19].*

III. Sub-Nyquist USF in Practice

Theorem 1 in Section II provides solutions for spectral estimation via sub-Nyquist Unlimited Sampling Framework. However, signal recovery with a theoretical guarantee in the presence of bounded noise has not been pursued, which is particularly critical in real-world scenarios as quantization induces bounded error. This may compromise the HDR capability of the sub-Nyquist `USF` method stated in Section II, necessitating a more *robust* sampling architecture and recovery approach.

Robust Multi-Channel Sub-Nyquist `USF`. Let $g(t)$ be a sum of K complex exponentials which is real-valued. The multi-channel sampling architecture illustrated in Fig. 2 implements real-valued modulo thresholds. The thresholds $\beta_l = \epsilon c_l/2,\ l = 0, 1$ are scaled integers, where $\mathtt{GCD}(c_0, c_1) = 1, c_0, c_1 \in \mathbb{Z}^+$ and $\epsilon \in \mathbb{R}^+$. The new architecture is more robust to noise, which gives rise to the multi-channel folded measurements given by

$$\begin{cases} u_0[n] = \mathscr{M}_{\beta_0}(g[n]) & u_1[n] = \mathscr{M}_{\beta_1}(g[n]) \\ u_2[n] = \mathscr{M}_{\beta_0}(g_{T_d}[n]) & u_3[n] = \mathscr{M}_{\beta_1}(g_{T_d}[n]) \end{cases}. \tag{7}$$

In the presence of bounded noise $\eta_l[n]$, given noisy folded measurements $\overline{u}_l[n] = u_l[n] + \eta_l[n], n \in \mathbb{I}_{N_l}, l \in \mathbb{I}_4$. Our goal again is to retrieve the $2K$ unknowns $\{c_k, f_k\}_{k=0}^{K-1}$.

RCRT-based Sub-Nyquist `USF` Spectral Estimation. RCRT can be used to determine the modular multiplicative inverse, which provides theoretical guarantee against bounded noise. Given the same specification, however, the performance bounds provided by the new architecture Fig. 2 is $\sqrt{2}\times$ higher compared to the previous sampling scheme as shown in Corollary 2. This can result in one quantization bit difference. We follow the same decoupling and unfolding strategy described in Section II, the input signals are *pairwise common to all channels*, for which their combinations lead to a system of congruence equations,

$$g[n] = 2\beta_0 a_0[n] + u_0[n], \quad g[n] = 2\beta_1 a_1[n] + u_1[n] \tag{8}$$

where $\{a_0[n], a_1[n]\}_{n\in\mathbb{I}_N} \in \mathbb{Z}^2$, while the frequency unfolding is the same as what has been presented in Theorem 1.

Based on the result above, we have the following theorem:

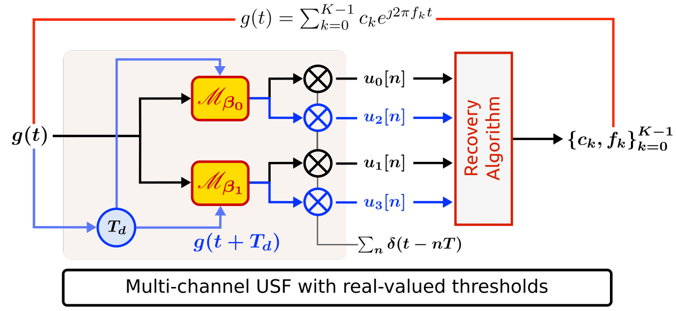

Fig. 2. USF acquisition architecture with real-valued thresholds that allows sub-Nyquist frequency estimation.

Theorem 2. *Let $g(t) = \sum_{k=0}^{K-1} c_k e^{\jmath\omega_k t}$. Given noisy modulo measurements $\{\overline{u}_l\}_{n\in\mathbb{I}_{N_i}}^{l\in\mathbb{I}_4}$, then, the reconstruction $\widetilde{g}[n]$ of $g[n]$ can be achieved with $N_i \geqslant \left(2 - \left\lfloor \frac{i}{2} \right\rfloor\right) K, i \in \mathbb{I}_4$ samples up to an error bounded by $\|g - \widetilde{g}\|_\infty < \|\eta_l\|_\infty = \epsilon/4$, provided that $T_d \leqslant \frac{\pi}{\max_k |\omega_k|}$ and $\|g(t)\|_\infty < \epsilon \mathtt{LCM}(c_0, c_1)/2$.*

Proof. Similar to the strategy in Section II, we sequentially perform unfolding in amplitude and frequency domain.

Amplitude Unfolding. The key idea of robust signal recovery is that, the modular multiplicative inverse estimation is exact due to the integer constraints, provided that the noise is upper bounded. Namely, $\mathscr{Q}(\Gamma + \varepsilon) = \mathscr{Q}(\Gamma), \Gamma \in \mathbb{Z}$ if $|\varepsilon| < 1/2$. More specifically, re-organizing the congruence equations from the sampling architecture in Fig. 2 leads to [21],

$$\mathscr{Q}\left((\overline{u}_1[n] - \overline{u}_0[n])/\epsilon\right) = c_0 a_0[n] - c_1 a_1[n] \tag{9}$$

where $\{a_0[n], a_1[n]\} \in \mathbb{Z}^2$ can be determined via exhaustive search, provided that $\|g(t)\|_\infty < \epsilon \mathtt{LCM}(c_0, c_1)/2, c_0, c_1 \in \mathbb{Z}^+$. This implies that $\|\eta_l\|_\infty < \epsilon/4, l \in \mathbb{I}_2$. As for the frequency unfolding, we utilize the same strategy stated in Section II. $\square$

In practice, this give rise to performance bounds of sub-Nyquist `USF` spectral estimation in the presence of quantization error. Taking a step further, we reveal the interplay between the bit budget, error bounds and dynamic range gain:

Corollary 1. *Let $g(t) = \sum_{k=0}^{K-1} c_k e^{\jmath\omega_k t}$. Given quantized modulo measurements $\{\overline{u}_l[n]\}_{n\in\mathbb{I}_{N_l}}^{l\in\mathbb{I}_4}$, then, the reconstruction $\widetilde{g}[n]$ of $g[n]$ can be achieved with $4K$ samples up to an error upper bounded by $\|g - \widetilde{g}\|_\infty < \epsilon c/2^{B+1}$, provided that $T_d \leqslant \frac{\pi}{\max_k |\omega_k|}$, $\|g(t)\|_\infty < \epsilon \mathtt{LCM}(c_0, c_1)/2$ and*

$$B > \log_2(c) + 1 \tag{10}$$

where $B \in \mathbb{Z}^+$ is the quantization bit budget and $c \stackrel{\text{def}}{=} \|c_k\|_\infty$.

Proof. The corollary holds as long as the quantization step, $2\beta_{\max}/2^B$ where $\beta_{\max} = \|\beta_k\|_\infty$, is smaller than the critical threshold $\epsilon/2$, resulting in the inequality in (10). $\square$

We compare the robustness of schemes in Fig. 1 and Fig. 2:

Corollary 2. *Let $g(t) = \sum_{k=0}^{K-1} c_k e^{\jmath\omega_k t}$. Given quantized modulo measurements $\{\overline{v}_l[n] = v_l[n] + \zeta_l[n]\}_{n\in\mathbb{I}_{N_l}}^{l\in\mathbb{I}_4}$, where $\zeta_l[n]$ is bounded noise, then, the reconstruction $\widetilde{g}[n]$ of $g[n]$*

Algorithm 1 USF Sub-Nyquist Frequency Estimation.

Input: $\{u_i[n]\}_{n\in\mathbb{I}_{N_i}}^{i\in\mathbb{I}_4}$ for $\beta \in R$

1: Unfold $g[n]$ and $g_{T_d}[n]$ based on (8).
2: Calculate aliased frequencies ν_k using (6).
3: Use least squares to obtain estimates of c_k.
4: Use least squares to find the phase term $e^{\jmath 2\pi f_k T_d}$ of (6).

Output: Signal parameters $\{f_k, c_k\}_{k=0}^{K-1}$.

TABLE I
USF SUB-NYQUIST SAMPLING SIMULATION

Complex-valued threshold								
Exp. No.	N	f_s (Hz)	T_d (μs)	ϵ	ρ	$\|\|g\|\|_\infty$	f_k (Hz)	MSE(f_k, $\hat{f}_k$)
1	29	1	1	0.01	0.361	26	[100.09, 142.30, 172.15]	6.73×10^{-29}
2	29	1	1	0.01	0.361	26	[1206.30, 1224.64, 1870.98]	6.89×10^{-26}
3	29	1	1	0.01	0.361	26	[10102.11, 14956.64, 15018.73]	4.41×10^{-24}
Robust Multi-Channel Sub-Nyquist USF								
Exp. No.	N	f_s (Hz)	T_d (μs)	λ_1	λ_2	$\|\|g\|\|_\infty$	f_k (Hz)	MSE(f_k, $\hat{f}_k$)
1	29	1	1	0.310	0.315	19	[100.09, 142.30, 172.15]	6.73×10^{-29}
2	29	1	1	0.310	0.315	19	[1206.30, 1224.64, 1870.98]	1.72×10^{-26}
3	29	1	1	0.310	0.315	19	[10102.11, 14956.64, 15018.73]	1.10×10^{-24}

can be achieved with $4K$ samples up to an error bounded by $\|g - \widetilde{g}\|_\infty < 2\sqrt{2}\rho/2^{B+1}$, provided that $T_d \leqslant \frac{\pi}{\max_k |\omega_k|}$, $\|g(t)\|_\infty < \epsilon\sqrt{p^2+q^2}/2$ and

$$B > \log_2\left(\sqrt{p^2+q^2}\right) + 1.5. \tag{11}$$

Given a fixed signal dynamic range, *i.e.*, $\|g(t)\|_\infty = \text{const}$, Corollary 2 reveals that the sampling architecture in Fig. 2 requires fewer bits. This leads to a more robust signal recovery in practice when the bit budget is limited due to power constraints.

Recovery Approach. The proposed reconstruction method, outlined in Algorithm 1, involves two phases: amplitude unfolding and frequency unfolding. This study introduces two USF architectures based on different types of modulo thresholds. The first architecture utilizes complex-valued thresholds, benefiting from the use of modulo ADCs with identical thresholds. In contrast, the architecture with real-valued thresholds employs varying modulo thresholds, offering greater resilience to quantization noise.

IV. NUMERICAL EXPERIMENTS

We perform numerical experiments to validate the performance of two approaches mentioned above in both noiseless and noisy conditions. We tabulate the experimental parameters and results in Table I. In noiseless scenarios, we can achieve signal recovery up to machine precision and dynamic range gains up to $72\times$ (Fig. 1) and $60\times$ (Fig. 2).

In the presence of quantization, we conduct experiments under different quantization bits, ranging from 4 bits to 12 bits, to assess the frequency estimation, as shown in Fig. 3 and Fig. 4. Each dot ("•") represents one estimate (from the total of ten trials for each bit-budget). The input signal consists of three real-valued sinusoids. For each trial, the ratio of amplitudes was changed ensuring $\|g\|_\infty$ remains fixed. We show that a sufficiently accurate frequency estimation can be achieved from

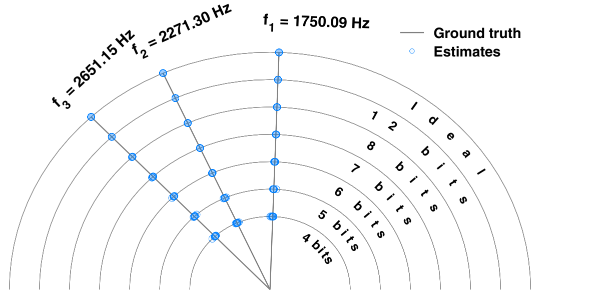

Fig. 3. Sub-Nyquist Sampling with complex-valued thresholds – $p = 5$, $q = 2$, $\epsilon = 1$, $\rho = 2.693$, $f_s = 1$Hz, $T_d = 1/6000$s, and $||g||_\infty = 14.45$

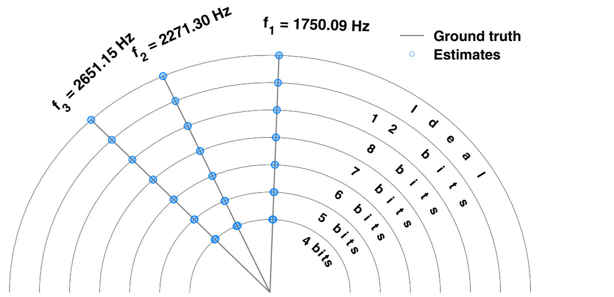

Fig. 4. Sub-Nyquist Sampling with real-valued thresholds – $\lambda_1 = 3$, $\lambda_2 = 3.5$, $\epsilon = 1$, $f_s = 1$Hz, $T_d = 1/6000$s and $||g||_\infty = 20.95$.

TABLE II
ENOB PER CHANNEL

Quant. bits	Complex-valued threshold (ENOB)				Real-valued threshold (ENOB)			
	v_0	v_1	v_2	v_3	u_0	u_1	u_2	u_3
4	3.674	3.647	3.727	3.736	3.732	3.684	3.676	3.636
5	4.716	4.703	4.695	4.720	4.782	4.661	4.703	4.607
6	5.748	5.776	5.669	5.739	5.852	5.679	5.679	5.602
7	6.766	6.682	6.718	6.714	6.765	6.642	6.664	6.652
8	7.722	7.766	7.718	7.722	7.744	7.633	7.721	7.628
12	11.724	11.724	11.726	11.751	11.768	11.714	11.727	11.600

as few as 4-bit quantization and $6\times$ DR improvement. We calculate the Effective Number of Bits (ENOB) [22]

$$\mathsf{ENOB} = \frac{\mathsf{SINAD} - 1.76}{6.02}, \ \mathsf{SINAD} = 10\log_{10}\left(\frac{P_s + P_n}{P_n}\right)$$

where P_s and P_n are the signal and noise power, respectively. We document the results in Table II, showcasing the robustness of the proposed sub-Nyquist USF method against bounded noise.

V. CONCLUSION

In this paper, we propose a novel multi-channel USF pipeline that allows for exact frequency estimation without any sampling rate requirement. We introduce two sampling architectures and derive the performance bounds in the presence of bounded noise (*e.g.* quantization noise). Numerical validation of our approaches agrees with the theoretical advantages deduced from our analysis. Practical implementation of the sampling strategy, as well as recovery algorithms in an efficient fashion, remains an interesting future pursuit.

REFERENCES

[1] E. Robinson, “A historical perspective of spectrum estimation,” *Proc. IEEE*, vol. 70, no. 9, pp. 885–907, Sep. 1982.

[2] P. Stoica and R. L. Moses, *Spectral analysis of signals*, 1st ed. Pearson Prentice Hall, 2005.

[3] P. P. Vaidyanathan and P. Pal, “Sparse Sensing With Co-Prime Samplers and Arrays,” *IEEE Trans. Sig. Proc.*, vol. 59, no. 2, pp. 573–586, 2011.

[4] S. Qin, Y. D. Zhang, M. G. Amin, and A. Zoubir, “Generalized coprime sampling of Toeplitz matrices,” in *Proc. IEEE Int. Conf. Acoust., Speech, Sig. Proc.*, 2016, pp. 4468–4472.

[5] X. Li, H. Liang, and X.-G. Xia, “A Robust Chinese Remainder Theorem With Its Applications in Frequency Estimation From Undersampled Waveforms,” *IEEE Trans. Sig. Proc.*, vol. 57, no. 11, pp. 4314–4322, 2009.

[6] A. Bhandari, F. Krahmer, and R. Raskar, “On Unlimited Sampling and Reconstruction,” *IEEE Trans. Sig. Proc.*, vol. 69, pp. 3827–3839, 2021.

[7] A. Bhandari, F. Krahmer, and T. Poskitt, “Unlimited Sampling From Theory to Practice: Fourier-Prony Recovery and Prototype ADC,” *IEEE Trans. Sig. Proc.*, vol. 70, pp. 1131–1141, 2022.

[8] A. Weiss, E. Huang, O. Ordentlich, and G. W. Wornell, “Blind Modulo Analog-to-Digital Conversion,” *IEEE Trans. Sig. Proc.*, vol. 70, pp. 4586–4601, 2022.

[9] D. Florescu, F. Krahmer, and A. Bhandari, “The Surprising Benefits of Hysteresis in Unlimited Sampling: Theory, Algorithms and Experiments,” *IEEE Trans. Sig. Proc.*, vol. 70, pp. 616–630, 2022.

[10] R. Guo and A. Bhandari, “ITER-SIS: Robust Unlimited Sampling Via Iterative Signal Sieving,” in *Proc. IEEE Int. Conf. Acoust., Speech, Sig. Proc.*, 2023, pp. 1–5.

[11] A. Bhandari, F. Krahmer, and R. Raskar, “Unlimited Sampling of Sparse Sinusoidal Mixtures,” in *2018 IEEE International Symposium on Information Theory (ISIT)*, 2018, pp. 336–340.

[12] ——, “Unlimited Sampling of Sparse Signals,” in *Proc. IEEE Int. Conf. Acoust., Speech, Sig. Proc.*, 2018, pp. 4569–4573.

[13] D. Prasanna, C. Sriram, and C. R. Murthy, “On the Identifiability of Sparse Vectors From Modulo Compressed sensing measurements,” *IEEE Signal Process. Lett.*, vol. 28, pp. 131–134, 2021.

[14] A. Bhandari, “Back in the US-SR: Unlimited Sampling and Sparse Super-Resolution with Its Hardware Validation,” *IEEE Signal Process. Lett.*, vol. 29, pp. 1047–1051, 2022.

[15] L. Gan and H. Liu, “High Dynamic Range Sensing Using Multi-Channel Modulo Samplers,” in *IEEE 11th Sensor Array and Multichannel Signal Processing Workshop (SAM)*, 2020, pp. 1–5.

[16] Y. Gong, L. Gan, and H. Liu, “Multi-Channel Modulo Samplers Constructed From Gaussian Integers,” *IEEE Signal Process. Lett.*, vol. 28, pp. 1828–1832, 2021.

[17] R. Guo and A. Bhandari, “Unlimited Sampling of FRI Signals Independent of Sampling Rate,” in *Proc. IEEE Int. Conf. Acoust., Speech, Sig. Proc.*, 2023, pp. 1–5.

[18] W. Yan, L. Gan, S. Hu, and H. Liu, “Towards optimized multi-channel modulo-adcs: Moduli selection strategies and bit depth analysis,” in *Proc. IEEE Int. Conf. Acoust., Speech, Sig. Proc.*, 2024, pp. 9496–9500.

[19] Y. Zhu, R. Guo, P. Zhang, and A. Bhandari, “Frequency Estimation via Sub-Nyquist Unlimited Sampling,” in *Proc. IEEE Int. Conf. Acoust., Speech, Sig. Proc.*, Apr. 2024, pp. 9636–9640.

[20] L. Xiao and X.-G. Xia, “Frequency determination from truly sub-Nyquist samplers based on robust Chinese remainder theorem,” *Signal Process*, vol. 150, pp. 248–258, 2018.

[21] W. Wang and X.-G. Xia, “A Closed-Form Robust Chinese Remainder Theorem and Its Performance Analysis,” *IEEE Trans. Sig. Proc.*, vol. 58, no. 11, pp. 5655–5666, 2010.

[22] W. Kester, “Understand SINAD, ENOB, SNR, THD, THD + N, and SFDR so You Don’t Get Lost in the Noise Floor (MT-003 Tutorial),” Analog Devices, Tech. Rep. MT-003, 2009.